Optics Letters

Fast and accurate waveform modeling based on sequence-to-sequence framework for multi-channel and high-rate optical fiber transmission

Minghui Shi,[1] Zekun Niu,[1,2] Hang Yang,[1] Junzhe Xiao,[1] Chuyan Zeng,[1] Yunfan Zhang,[1] Zhixiong Zheng,[1] Weisheng Hu,[1] and Lilin Yi[1,*]

[1]State Key Lab of Advanced Communication Systems and Networks, School of Electronic Information and Electrical Engineering, Shanghai Jiao Tong University, Shanghai 200240, China
[2]zekunniu@sjtu.edu.cn
*lilinyi@sjtu.edu.cn

Received 16 January 2025; revised 22 February 2025; accepted 24 February 2025; posted 25 February 2025; published 24 March 2025

We propose a sequence-to-sequence (Seq2Seq) framework integrated with a feature decouple distributed (FDD) method for fast and accurate channel waveform modeling in multi-channel, high-rate wavelength-division multiplexing (WDM) optical fiber transmission. This framework enables the simultaneous prediction of multiple output symbols in a single inference, dramatically reducing the repeated calculation of adjacent padding symbols and achieving a significant reduction in time complexity compared to the traditional split-step Fourier method (SSFM). Additionally, transfer learning is leveraged to streamline the training process and improve the accuracy of the Seq2Seq architecture. In a 40-channel, 140 GBaud WDM system, Seq2Seq-FDD reduces computation time to a mere 0.22% of that required by the variable step size SSFM. In a five-channel configuration, Seq2Seq-FDD achieves an 85.5% improvement in NMSE over simplified FDD-Co-LSTM and a 99.88% reduction in computation time compared to vanilla-FDD. This framework provides a highly efficient solution for waveform modeling in multi-channel, high-rate WDM systems.

https://doi.org/10.1364/OL.555880

Introduction. Optical fiber communication forms the backbone of modern information transmission systems. Fast and accurate modeling and simulation of optical fiber channels are pivotal in optimizing optical networks [1], advancing digital signal processing (DSP) algorithms [2], and performing end-to-end (E2E) optimization [3].

The evolution of optical pulses within fiber channels is governed by the nonlinear Schrödinger equation (NLSE) [4]. Gaussian noise (GN) [5] and enhanced GN (EGN) [6] models offer fast channel modeling by focusing on power-level results and accurately estimating the generalized signal-to-noise ratio (GSNR). However, the GN-like models fail to provide waveform information, limited waveform-level application such as advancing DSP algorithms. The split-step Fourier method (SSFM) [4] provides accurate waveform results by solving linear and nonlinear operators separately in each small fiber segment. While SSFM is effective, it incurs significant iterative computation, particularly in multi-channel and high-rate wavelength-division multiplexing (WDM) systems [7].

Recently, deep learning (DL) has emerged as a promising approach for optical fiber channel waveform modeling [8–15], owing to its superior nonlinear fitting capabilities and efficient parallel computation. Innovations such as bidirectional long short-term memory (Bi-LSTM) [8], generative adversarial network (GAN) [9], multi-head attention [10] and Fourier neural operator (FNO) [11] have been applied to signal-channel systems. Additionally, Bi-LSTM combined with feature decoupled distributed (vanilla-FDD) [12], and deep operator network (DeepONet) [13] have been extended to multi-channel waveform modeling. The simplified center-oriented LSTM integrated with FDD (FDD-Co-LSTM) [14] further reduced the complexity. Despite these advancements, DL-based fiber modeling that simultaneously achieve high accuracy and low complexity in multi-channel, high-rate WDM systems remains a challenge [16], particularly due to stronger linear effects, which lead to exponentially growing inter-symbol interference (ISI). While the FDD employs a physical model to address linear effects, the residual nonlinear inter-symbol correlations remain long, as linear and nonlinear effects occur simultaneously and interact within the fiber channel.

In this Letter, we introduce a sequence-to-sequence (Seq2Seq) framework combined with an FDD method to achieve fast and accurate fiber channel waveform modeling under multi-channel, high-rate WDM systems. This framework employs a multiple-symbol output approach per inference, significantly reducing the repeated calculation compared to single-symbol predictions per inference. Transfer learning is employed to streamline the training process of the Bi-LSTM with hundreds of cells, enhancing both efficiency and accuracy of the Seq2Seq. In a 40-channel 140 GBaud system, the computation time of Seq2Seq-FDD is reduced to just 0.22% of that required by variable step size SSFM. Furthermore, in a five-channel case, Seq2Seq-FDD achieves an 85.5% improvement in NMSE over simplified

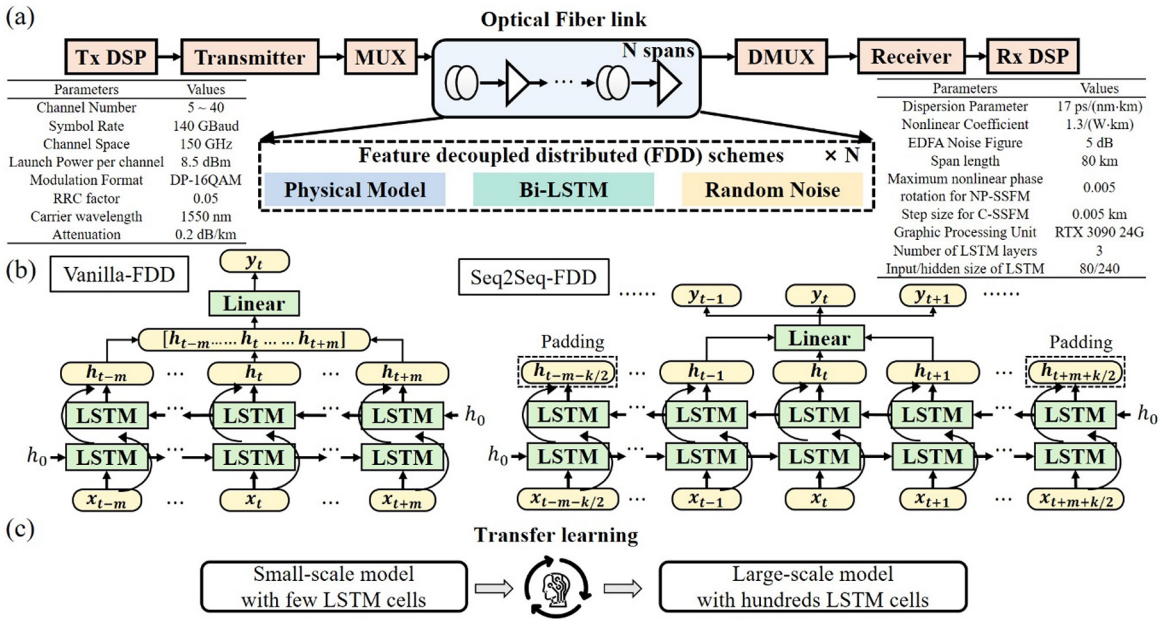

Fig. 1. (a) The structure and parameters of optical fiber transmission WDM simulation systems and feature decoupled distributed schemes. (b) The structure of Bi-LSTM employed in vanilla-FDD and Seq2Seq-FDD. (c) The processing of transfer learning to implement Seq2Seq framework.

FDD-Co-LSTM and a 99.88% reduction in computation time compared to vanilla-FDD.

Principle. Fiber channel modeling, governed by the NLSE [4], involves both linear and nonlinear operators. The linear effects lead to long ISI and nonlinear inter-symbol correlations, particularly in multi-channel and high-rate systems, necessitating the consideration of preceding and subsequent symbols' influence on the current symbols during fiber channel modeling. Seq2Seq-FDD is proposed to enhance the accuracy and reduce the complexity, as shown in Figs. 1(a) and 1(b). FDD combines a physical model and a Bi-LSTM to model single-span optical fiber channel, with the physical model addressing linear effects and the Bi-LSTM capturing nonlinear effects. ASE noise introduced by erbium-doped fiber amplifier (EDFA) is added based on Gaussian distributions. To achieve long-haul transmission, multiple FDD modules are cascaded. To account for nonlinear inter-symbols correlations, the input window of the Bi-LSTM comprises $2m + k$ symbols, where k central symbols are predicted, and m preceding and subsequent symbols provide adjacent nonlinear information. In vanilla-FDD, k is set to 1, while $2m$ symbols are padding symbols, resulting in a significant repeated computation. For a transmitted signal with N symbols, vanilla-FDD requires N cycles to predict the entire signal, leading to high computational complexity. To overcome this limitation, the Seq2Seq framework adopts a multiple-symbol input and multiple-symbol output approach. Specifically, the number of central symbols k is set to several thousands (much larger than m), enabling the prediction of thousands of symbols. This drastically reduces repeated computation to a ratio of $2m/k$, far lower than the $2m$ ratio in vanilla-FDD. The simplified FDD-Co-LSTM introduced this multiple-symbol output method to mitigate high computational complexity. However, FDD-Co-LSTM applies this approach only during inference, while the training process employs a single-symbol output approach, potentially causing parameter mismatch and degrading the accuracy of nonlinear modeling during multi-symbol output. The Bi-LSTM in the multiple-symbol output method contains thousands of LSTM cells, which pose challenges due to excessive dataset sizes and significant computational resource requirement to directly train such large-scale models. The Seq2Seq framework combined with transfer learning overcomes this challenge through a two-stage training process, as depicted in Fig. 1(c). In the first stage, a small-scale Bi-LSTM with small k and m values (both set to 20 in this study) is trained to capture the dominant nonlinear effects from most adjacent symbols while minimizing training resource usage. In the second stage, the small-scale Bi-LSTM is fine-tuned into a large-scale Bi-LSTM, where k is set to hundreds or thousands, allowing the model to capture residual nonlinearities from distant symbols. Transfer learning facilitates this process, allowing the model to effectively learn the influence of nearby symbols while still accounting for the effects of more distant ones, thereby enhancing accuracy.

We construct an SSFM-based optical fiber transmission simulation system to generate the dataset, with its structure and parameters illustrated in Fig. 1(a). The sampling rate in SSFM is four times the channel number. The step size of the SSFM is determined using a maximum nonlinear phase rotation method to balance accuracy and complexity, which is referred to as NP-SSFM. The constant step SSFM is called C-SSFM. The data collection and preprocessing process follows the design outlined in [15], with additional details of the model training provided in Supplement 1.

Results. To demonstrate the efficiency of transfer learning in implementing Seq2Seq-FDD, Fig. 2 shows the loss curves for the two-stage training process. In the first stage, the small-scale model requires more iterations to learn the primary nonlinear influence. Building upon this foundation, the model in the second stage effectively captures the residual nonlinear effects from

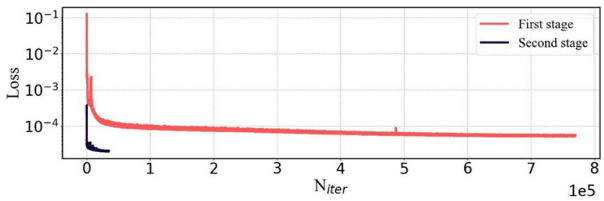

Fig. 2. Loss curves for two-stage training processing.

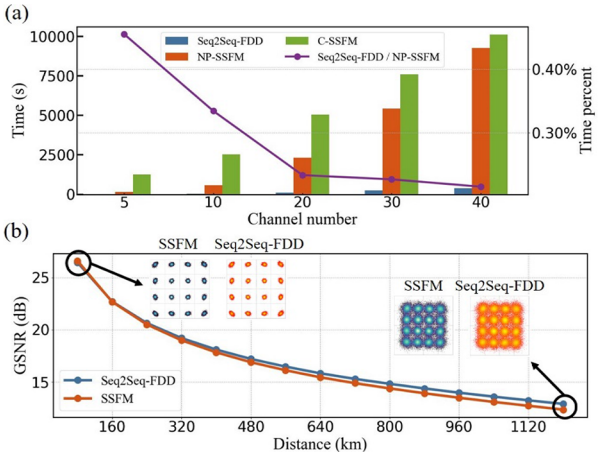

Fig. 3. (a) Computational complexity as a function of channel number. The left axis represents the absolute time changes, while the left axis shows the time percent of Seq2Seq-FDD relative to NP-SSFM. (b) GSRN versus distances and constellations of Seq2Seq-FDD and NP-SSFM.

distinct symbols with only 4.5% of the iterations required in the first stage, significantly reducing training resource consumption.

The computational complexity of Seq2Seq-FDD is distinctly demonstrated in comparison to SSFM. A signal with 10^6 symbols per channel is transmitted over an 80 km span. The computational complexity is shown in Fig. 3(a). In a five-channel WDM configuration, Seq2Seq-FDD achieves a computation time of just 0.66 s, compared to 145 s for NP-SSFM, and 1265 s for C-SSFM, representing nearly 200-fold and 2000-fold speedups over NP-SSFM and C-SSFM, respectively. The computational time advantage of Seq2Seq-FDD becomes even more pronounced in larger-channel configurations. The time percent of Seq2Seq-FDD relative to NP-SSFM achieves approximately 0.22% of NP-SSFM in a 40-channel configuration. These results underscore the significant reduction in computational complexity achieved by Seq2Seq-FDD compared with SSFM. We further evaluate the accuracy of Seq2Seq-FDD compared to SSFM. Figure 3(b) illustrates the GSNR curves and constellations for Seq2Seq-FDD and SSFM. The GSNR of both models remains nearly identical, and their constellations display comparable nonlinear phase rotations, validating the nonlinear modeling with high accuracy of Seq2Seq-FDD relative to SSFM.

To validate the waveform modeling capacity of Seq2Seq-FDD, the NMSE is calculated using Eq. (1), where N_{data} is the size of the data, y and y_i denote the outputs from SSFM and DL-based channel. We evaluate NMSE in a five-channel 140 GBaud WDM configuration, with each channel containing

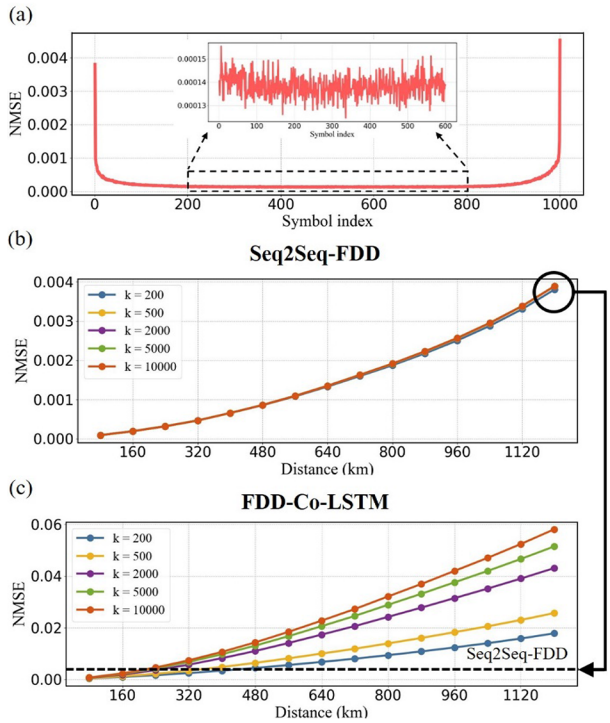

Fig. 4. (a) NMSE of Seq2Seq-FDD versus symbols at different positions. (b) NMSE of Seq2Seq-FDD versus distances of various central symbol numbers k. (c) NMSE of simplified FDD-Co-LSTM versus distances of various central symbol numbers k.

2.5×10^5 symbols as follows:

$$\text{NMSE} = \frac{\sum_{i-1}^{N_{\text{data}}} |\hat{y}_i - y_i|^2}{\sum_{i-1}^{N_{\text{data}}} |y_i|^2}. \tag{1}$$

Figure 4(a) displays the NMSE for output symbols across all positions when $m = 0$ and $k = 1000$, meaning no padding symbols. Central symbols achieve significantly lower NMSE, while approximately 200 preceding and succeeding symbols exhibit NMSE degradation due to insufficient adjacent symbols to capture nonlinear inter-symbol correlations effectively. The ISI caused by CD is roughly 570 preceding and succeeding symbols, indicating that FDD reduces the dependency on adjacent symbols by decoupling linear effects. To ensure accuracy, 400 padding symbols are required during testing in this Letter. We denote that the number of central symbols k in Seq2Seq-FDD is highly flexible and not constrained by the training dataset. Figures 4(b) and 4(c) show NMSE curves of Seq2Seq-FDD and FDD-Co-LSTM with various values of k across 1200 km transmission. The NMSE of Seq2Seq-FDD remains stable as k increases, even though the model is trained with $k = 600$. Conversely, the NMSE of FDD-Co-LSTM deteriorates with larger k, reflecting its inability to handle multiple-symbol outputs effectively. This deficiency stems from FDD-Co-LSTM being trained exclusively for $k = 1$, leading to parameter mismatches when k increases during inference. In contrast, Seq2Seq-FDD, trained with k in the hundreds, leverages the Bi-LSTM's memory and forget gate mechanisms to adapt seamlessly to multiple-symbols output. This enables flexible extension to larger k values while maintaining accuracy and reducing the complexity.

To further assess the advantages of Seq2Seq-FDD, we compare it to vanilla-FDD [12] and simplified FDD-Co-LSTM [14],

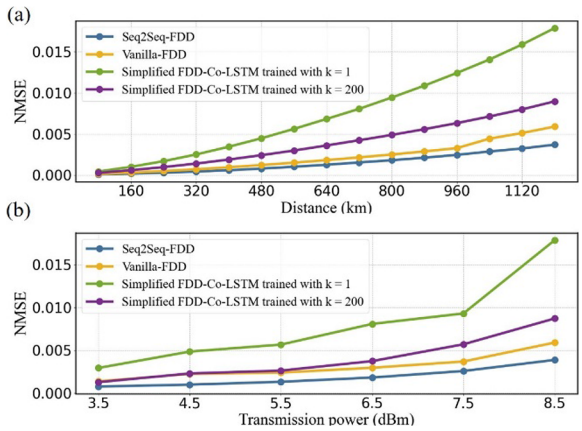

Fig. 5. (a) NMSE versus distances of Seq2Seq-FDD, vanilla-FDD and simplified FDD-Co-LSTM. (b) NMSE versus various transmission powers of Seq2Seq-FDD, vanilla-FDD, and simplified FDD-Co-LSTM after a 1200 km transmission.

Table 1. Times of Various DL Models

	Seq2Seq-FDD	Vanilla-FDD	Simplified FDD-Co-LSTM	NP-SSFM
Times (s)	**0.66**	120	0.96	145

trained with $k = 1$ and $k = 200$ and tested with $k = 200$. Figure 5(a) shows the NMSE curves for all models across a 1200 km transmission. At the 1200 km transmission, Seq2Seq-FDD achieves an NMSE of 3.7E-3, outperforming both vanilla-FDD and simplified FDD-Co-LSTM. Figure 5(b) shows the NMSE versus different launch powers after the 1200 km transmission, where Seq2Seq-FDD consistently achieves the lowest NMSE across various transmission powers, demonstrating its adaptability to different levels of nonlinearity. Simplified FDD-Co-LSTM trained with $k = 1$ suffers a degradation in accuracy due to parameter mismatches between training and testing. Both simplified FDD-Co-LSTM trained with $k = 200$ and vanilla-FDD employ a one-stage training process, which struggles to capture the nonlinear effects effectively due to the challenges of training large-scale models. In contrast, Seq2Seq-FDD utilizes a two-stage training approach, where the small-scale model in the first stage captures nearby nonlinear features effectively, and fine-tuning in the second stage improves results by better capturing distant nonlinear effects. Furthermore, Seq2Seq-FDD still maintains high accuracy across other symbol rates, as detailed in Supplement 1. Table 1 shows the computation times of three DL models over an 80 km transmission. Seq2Seq-FDD achieves the lowest computation time of just 0.66 s, demonstrating its efficiency in reducing computational complexity and addressing the extended ISI challenge through its multiple-symbol output design.

The advantage of Seq2Seq-FDD underlines its strong ability to model complex fiber channel's properties. We speculate that it is suitable for modeling not only wideband simulation systems but also for other optical systems governed by the NLSE, such as physical experimental system modeling [17] and ultrafast nonlinear dynamics prediction [18].

Conclusion. We propose a Seq2Seq framework combined with the FDD method for fast and accurate fiber channel waveform modeling. In a five-channel WDM configuration, Seq2Seq-FDD achieves an 85.5% improvement in NMSE over simplified FDD-Co-LSTM and a 99.88% reduction in computation time compared to vanilla-FDD. We believe this work paves the way for broader application of DL-based optical fiber channel waveform modeling.

Funding. National Key Research and Development Program of China (2023YFB2905400); National Natural Science Foundation of China (62025503); Shanghai Jiao Tong University 2030 Initiative.

Disclosures. The authors declare no conflicts of interest.

Data availability. Data underlying the results presented in this paper are not publicly available at this time but may be obtained from the authors upon reasonable request.

Supplemental document. See Supplement 1 for supporting content.

REFERENCES

1. Y. Zhang, X. Pang, Y. Song, *et al.*, J. Lightwave Technol. **42**, 95 (2024).
2. A. Napoli, Z. Maalej, V. A. J. M. Sleiffer, *et al.*, J. Lightwave Technol. **32**, 1351 (2014).
3. Z. Niu, H. Yang, H. Zhao, *et al.*, J. Lightwave Technol. **40**, 2807 (2022).
4. G. P. Agrawal, *Nonlinear Fiber Optics* (Academic, 2006), p. 41.
5. P. Poggiolini, J. Lightwave Technol. **30**, 3857 (2012).
6. A. Carena, G. Bosco, V. Curri, *et al.*, Opt. Express **22**, 16335 (2014).
7. P. Serena, C. Lasagni, S. Musetti, *et al.*, J. Lightwave Technol. **38**, 1019 (2020).
8. D. Wang, Y. Song, J. Li, *et al.*, J. Lightwave Technol. **38**, 4730 (2020).
9. H. Yang, Z. Niu, S. Xiao, *et al.*, J. Lightwave Technol. **39**, 1322 (2021).
10. Y. Zang, Z. Yu, K. Xu, *et al.*, J. Lightwave Technol. **40**, 6347 (2022).
11. X. He, L. Yan, L. Jiang, *et al.*, J. Lightwave Technol. **41**, 2301 (2023).
12. H. Yang, Z. Niu, H. Zhao, *et al.*, J. Lightwave Technol. **40**, 4571 (2022).
13. X. Zhang, M. Zhang, Y. Song, *et al.*, J. Lightwave Technol. **41**, 6908 (2023).
14. J. Zheng, T. Zhang, F. Zhang, *et al.*, Opt. Lett. **49**, 1848 (2024).
15. M. Shi, H. Yang, Z. Niu, *et al.*, in *2023 Asia Commun. Photonics Conf.* (Wuhan, China, 2023), p. 1.
16. M. Shi, H. Yang, Z. Niu, *et al.*, "Deep Learning waveform modeling for wideband optical fiber channel transmission: challenges and potential solutions," arXiv (2025).
17. H. Yang, Z. Niu, Q. Fan, *et al.*, Laser Photonics Rev. **18**, 2400234 (2024).
18. H. Yang, H. Zhao, Z. Niu, *et al.*, Opt. Express **30**, 43691 (2022).